Available online at www.sciencedirect.com
ScienceDirect
Journal of Magnetism and Magnetic Materials 309 (2007) 15–19
Journal of magnetism and magnetic materials
www.elsevier.com/locate/jmmm

Magnetic field heating study of Fe-doped Au nanoparticles

Andy Wijaya[a], Katherine A. Brown[b], Joshua D. Alper[c], Kimberly Hamad-Schifferli[b,c,*]

[a]Department of Chemical Engineering, Massachusetts Institute of Technology, Cambridge, MA, USA
[b]Biological Engineering Division, Massachusetts Institute of Technology, Cambridge, MA, USA
[c]Department of Mechanical Engineering, Massachusetts Institute of Technology, Cambridge, MA, USA

Received 21 December 2005; received in revised form 29 March 2006
Available online 16 May 2006

Abstract

Fe-doped Au nanoparticles are ideal for biological applications over magnetic oxides due to their conjugation chemistry, optical properties, and surface chemistry. We present an AC magnetic field heating study of 8 nm Fe-doped Au nanoparticles which exhibit magnetic behavior. Magnetic heating experiments were performed on stable aqueous solutions of the nanoparticles at room temperature. The nanoparticles exhibit magnetic field heating, with a specific absorption rate (SAR) of 1.84 W/g at 40 MHz and $H = 100$ A/m. The frequency dependence of the heating follows general trends predicted by power loss equations and is similar to traditional materials.

PACS: 61.46.Df; 87.83.+a; 87.54.Br; 65.80.+n; 82.60.Qr

Keywords: Nanoparticles; Fe-doped Au; Hyperthermia; AC magnetic field heating

1. Introduction

Magnetic nanoparticles have found utility in numerous biological applications, including sensing [1], imaging [2], cancer therapy, drug delivery, and hyperthermia for tumor therapy [3,4]. Hyperthermia applications have traditionally utilized magnetic oxide nanoparticles, predominantly iron oxide [4]. This is due to the fact that many robust synthetic strategies exist for iron oxides and variants, which result in high quality, monodisperse and crystalline nanoparticles [5]. On the other hand, gold nanoparticles have been utilized extensively in biological applications such as sensing [6], tumor therapy [7] and control [8], due to the fact that they are easily conjugated to both DNA [9,10] and proteins [11]. One of the chief advantages of utilizing gold nanoparticles is their versatile surface chemistry, which permits their water solubility and flexibility in conjugation to biomolecules [9,12]. Furthermore, gold nanoparticles possess unique optical properties because they have a strong optical absorption that shift with changes in its chemical environment. Therefore, new materials for hyperthermia that combine the advantages of gold with those of magnetic materials are desirable. In order to make them utilizable for magnetic applications, gold nanoparticles need to display magnetic behavior. This has been achieved previously by coating iron or iron oxide nanoparticles with a gold shell [13]. However, synthesis of core-shell structures can be challenging, and the magnetic properties are similar to the uncoated iron oxide nanoparticles. We have explored an alternative to core-shell particles by doping Au nanoparticles with Fe atoms [14]. This results in water-soluble nanoparticles that are magnetic due to the presence of the Fe atoms. Here, we perform a magnetic field heating study of the Fe-doped Au nanoparticles to determine their feasibility for hyperthermia.

2. Materials and methods

Fe-doped Au nanoparticles were synthesized in water by a simple modification [14] of a standard synthesis for gold

*Corresponding author. Department of Mechanical Engineering and Biological Engineering Division, Massachusetts Institute of Technology, 77 Massachusetts Avenue, 56-341C, Cambridge, MA 02139, USA. Tel.: +1 617 452 2385.
E-mail address: schiffer@mit.edu (K. Hamad-Schifferli).

0304-8853/$ - see front matter © 2006 Elsevier B.V. All rights reserved.
doi:10.1016/j.jmmm.2006.04.014

nanoparticles [15]. In brief, $HAuCl_4$ and $FeCl_3$ were reduced in aqueous solution simultaneously in the presence of citric acid, tannic acid, and sodium carbonate at $T = 50\,^{\circ}C$ to nucleate Au nanoparticles doped with Fe. The nanoparticles were functionalized with the ligand bis (*p*-sulphonatophenyl) phenylphosphine dihydrate, dipotassium salt (BPS) by ligand exchange. The nanoparticles were purified from reagents and excess ligand by multiple precipitations with NaCl and centrifugation. They were re-suspended in water and further purified by agarose gel electrophoresis. Fig. 1a shows a TEM image of the sample deposited from water solutions onto ultra thin holey carbon coated copper grids (Ted Pella) and imaged by a JEOL 2010 FEG Analytical Electron Microscope. The TEM image reveals that the nanoparticles are well separated and not present in aggregates. In addition, the nanoparticles resulting from this synthesis are relatively monodisperse. A distribution of $\langle r \rangle = 3.9 \pm 0.5$ nm (histogram, Fig. 1b) was determined through analysis of TEM images containing approximately 175 nanoparticles. The Fe content of the nanoparticles was 1.8%, as measured by elemental analysis in STEM. The nanoparticles exhibited a surface plasmon resonance characteristic of gold nanoparticles with $\lambda_{max} = 523$ nm (not shown). Fe-doped Au nanoparticles are stable in aqueous solution for several days to weeks stored at room temperature and did not precipitate or show appreciable surface plasmon shifts, behaviors indicative of aggregation [16]. The Fe-doped Au nanoparticles are an inhomogeneous material, as Fe at low atomic% will segregate into clusters in the bulk solid [17]. This is in contrast with bulk AuFe alloys which are homogeneous.

Fe-doped nanoparticles exhibit magnetic behavior as measured by superconducting quantum interference device (SQUID) magnetometry using a Quantum Design DC Magnetic Property Measurement System (Fig. 2). The samples were characterized in the powder form, which was obtained by ethanol precipitation from solution. The nanoparticles seem to exhibit a small but finite magnetic hysteresis at 300 K (Fig. 2 inset), indicating that the nanoparticles are either ferromagnetic or superparamagnetic.

2.1. Magnetic heating

The Fe-doped Au nanoparticles could be heated in an alternating magnetic field. The experimental setup was similar to those used in the literature for hyperthermia evaluation [18,19]. Current was supplied to a coil of 25 turns, inside of which the sample was placed. Sample volume was 100 μl and concentration was 14 mg/ml (equal to 3.7 μM in moles of particles/l). The temperature of the sample was measured as a function of time by a fluorescent temperature probe (Luxtron). Currents were supplied by a

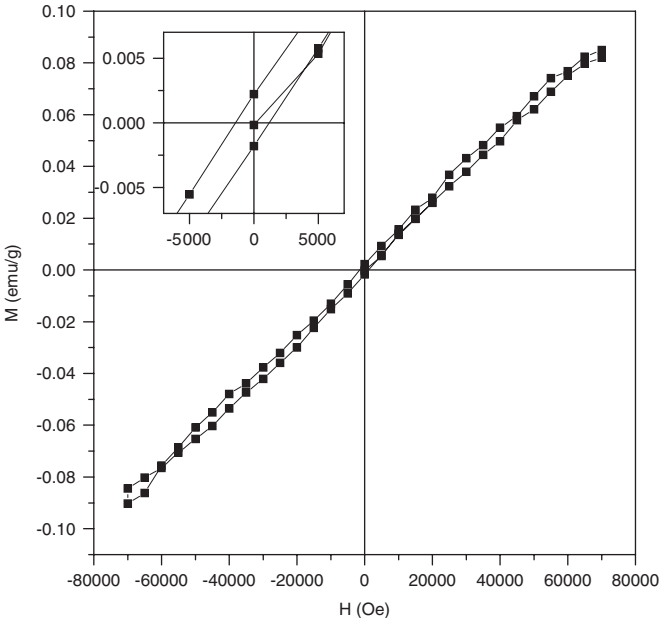

Fig. 2. SQUID data of Fe-doped Au NPs at 300 K. Inset: closeup of hysteresis region.

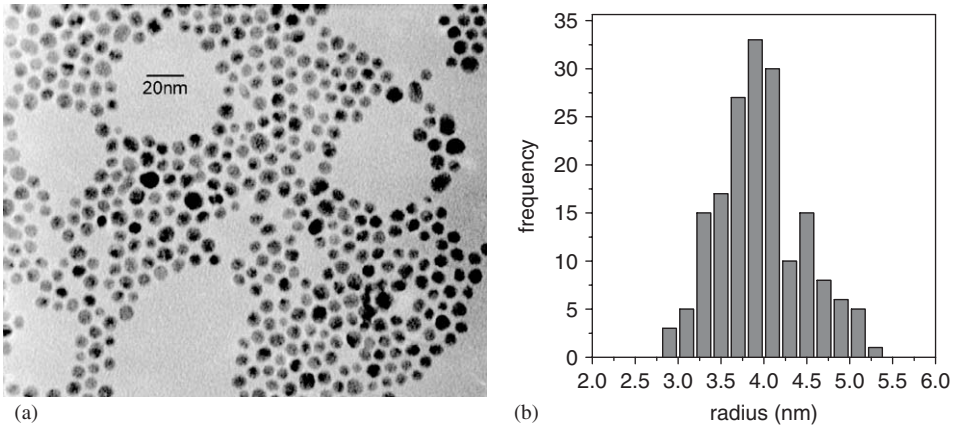

Fig. 1. (a) TEM of Fe-doped Au NPs, (b) histogram of sizes, $d> = 7.8 \pm 0.7$ nm.

signal generator (Hewlett Packard) amplified through a 100 W amplifier (Amplifier Research), in the frequency range of 100 kHz to 100 MHz. The field strength was calculated by measuring the current using a high-frequency current probe (Tektronix) and an oscilloscope (Agilent). Custom software (written in LabView) controlled the application of the signal and also measured the field strength and temperature. Due to the mismatch of the impedance, the current in the coil was obtained by combining frequency dependence circuit simulations in PSPICE (Personal computer Simulation Program with Integrated Circuits Emphasis) with the actual readings of the current probe.

The specific absorption rate (SAR) quantifies the rate of energy deposition in tissue in hyperthermia, which is a measure of the amount of energy converted by the magnetic particles from the magnetic field into heat per unit time and mass. Fig. 3 shows a typical SAR measurement of the Fe-doped Au nanoparticles. An alternating magnetic field of approximate field strength of 100 A/m at 40 MHz was applied between 100 s (t_i) and 400 s (dashed line). Upon application of the field, the measured temperature of the nanoparticle solution increased by 22 °C to reach a steady state value of 46 °C (solid line, curve labeled NP). The SAR of a magnetic fluid is determined by the initial linear temperature rise of a fluid measured after switching on the magnetic field:

$$\mathrm{SAR} = c\left.\frac{\mathrm{d}T}{\mathrm{d}t}\right|_{t=t_i}, \tag{1}$$

where c is the heat capacity of the sample, and $(\mathrm{d}T/\mathrm{d}t)_{t=t_i}$ is the initial slope of the temperature data. The SAR value was obtained from the data in Fig. 3 by fitting the rise to an exponential function based on the analytical solution of the boundary value problem for $T(t)$ of the sample [20]. The value of the initial slope was calculated by differentiating the exponential function with respect to time and solving at $t = t_i$. The c of the solution of Fe-doped Au nanoparticles was approximated by using a weighted average of the bulk values of c_{Au} and c_{water} (approximately 4.07 J/g K). The SAR was measured for a given field strength and frequency. Control experiments containing the nanoparticle ligand in aqueous solution, BPS were also investigated for magnetic field heating. The concentration of the BPS in the control solution was 1.93×10^{-4} M, approximately the same concentration at which they are present in the nanoparticle solution. The BPS showed negligible temperature increases (Fig. 3, solid line, curve labeled BPS). This illustrates that the heating observed is due to the Fe-doped Au nanoparticles and not the nanoparticle ligand or the solvent.

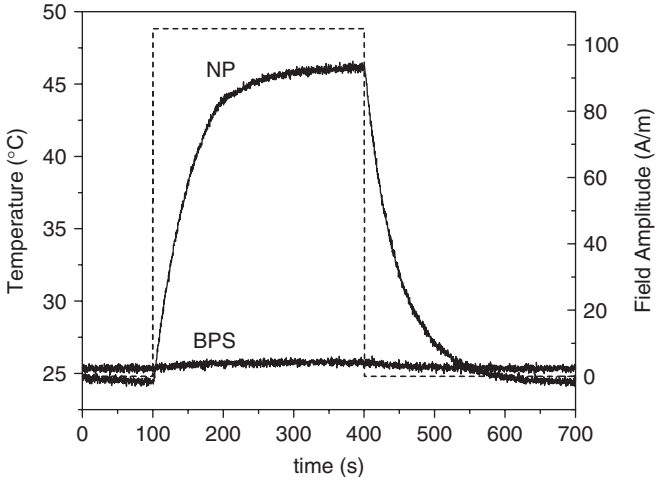

Fig. 3. SAR experiment of Fe-doped Au nanoparticles. A 40 MHz field of 100 A/m field strength is applied (dashed line) between 100 and 400 s. Temperature of a 3.7 μM solution of Fe-doped Au NPs (upper curve labeled NP) and a control solution of 193 μM BPS ligand (lower curve labeled BPS).

Usually SAR is described by power losses due to Brownian and Néel relaxation mechanisms [21,22]. The power dissipated by a nanoparticle can be described by

$$P = \frac{(mH\omega\tau_{\mathrm{eff}})^2}{2\tau_{\mathrm{eff}}k_{\mathrm{B}}TV(1+\omega^2\tau_{\mathrm{eff}}^2)}, \tag{2}$$

where m is the magnetic moment per particle, $\omega = 2\pi f$ the field frequency (radians/s), V the particle volume, and τ_{eff} the effective relaxation time. τ_{eff} depends on both Néel (τ_{N})and Brownian (τ_{B}) relaxation losses by

$$\tau_{\mathrm{eff}} = \frac{\tau_{\mathrm{N}}\tau_{\mathrm{B}}}{\tau_{\mathrm{N}}+\tau_{\mathrm{B}}}, \tag{3}$$

where the timescale of Brownian relaxation losses is

$$\tau_{\mathrm{B}} = \frac{8\pi\eta R_{\mathrm{H}}^3}{k_{\mathrm{B}}T}, \tag{4}$$

where η is the sample viscosity and R_{H} the particle hydrodynamic radius. Néel relaxation losses are described by

$$\tau_{\mathrm{N}} = \tau_0 \exp\frac{KV}{k_{\mathrm{B}}T}, \tag{5}$$

where $\tau_0 = 10^{-9}$ s is the relaxation time constant or frequency factor, K the anisotropy constant, and V the nanoparticle volume.

Therefore, to compare to the power loss equation, we performed magnetic heating at a range of frequencies (f). The power loss equation shows a square law field dependence so the SAR data was normalized to H^2. SAR/H^2 of the Fe-doped Au nanoparticles is plotted as a function of field frequency (Fig. 4a). The SAR of Fe-doped Au nanoparticles in Fig. 4a follows relaxation losses trends, where it is a square law dependent on frequency at lower frequencies, but frequency independent above some threshold [21]. This behavior is similar to that experimentally observed for Fe_3O_4 nanoparticles [23]. A simulated power loss curve for Fe-doped Au nanoparticles was generated (Fig. 4b) using Eq. (2). A magnetic moment of $3.3\,\mu_{\mathrm{B}}$/Fe atom [24] and $K = 8.5 \times 10^5$ J/m^3 from literature on FeAu thin film alloys was assumed [25]. The

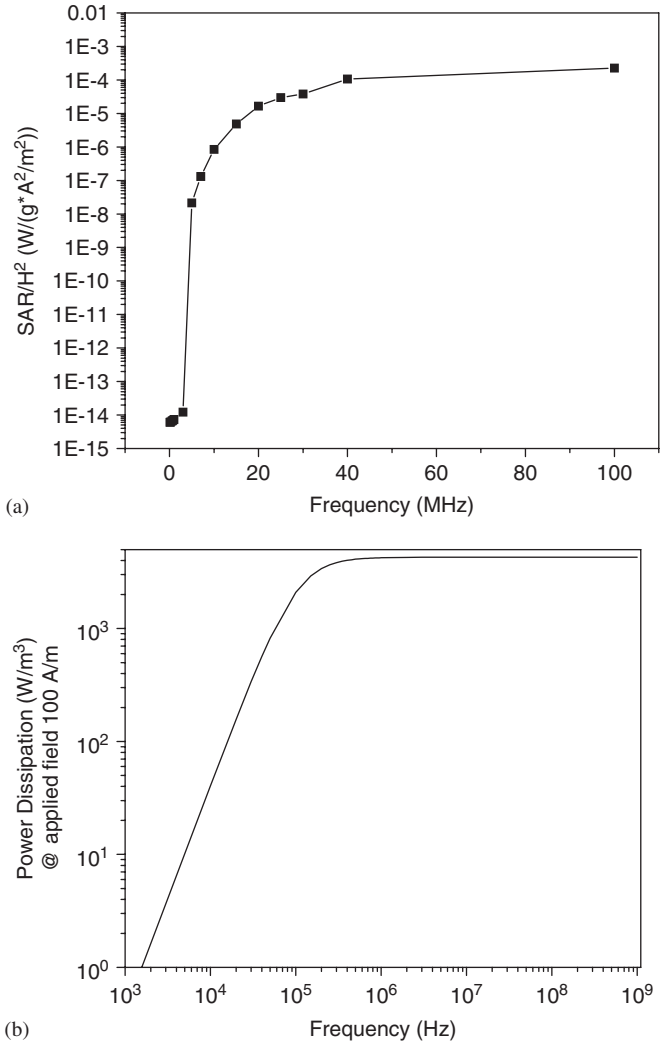

Fig. 4. (a) Frequency dependence of SAR normalized to H^2 of Fe-doped Au nanoparticles, (b) simulation of power losses for Fe-doped Au nanoparticles.

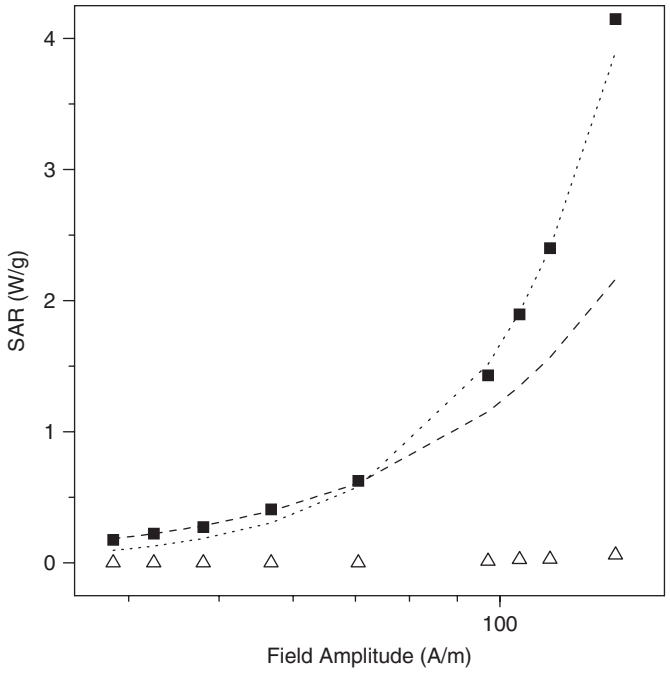

Fig. 5. SAR vs. field amplitude at 40 MHz for Fe-doped Au nanoparticles (squares). Control solution of the nanoparticle ligand, BPS (open triangles). Fit of the Fe-doped Au nanoparticles to SAR $\propto H^m$, shown, where $m = 2$ (dashed line) and $m = 3$(dotted line).

plot shows the general trend of SAR proportional to f^2 at low frequencies, and reaching plateau at higher frequencies. It should be noted that the frequency dependence at which SAR plateaus is extremely sensitive to the value of the anisotropy constant used in the calculation. Because of the lack of measured values of K for FeAu alloy nanoparticles, this limits us to use the value measured for thin films, and thus can be used only as an approximation.

SAR values of Fe-doped Au nanoparticles were measured as a function of field strength at a frequency of 40 MHz (Fig. 5). The magnetic field was varied from 40 to 135 A/m. At these field strengths, the Fe-doped Au nanoparticles have a SAR that ranges from 0 to 4 W/g (squares). Meanwhile, the control solution of the ligand (open triangles) shows a negligible SAR (~0 W/g), even at higher field strengths. SAR has been shown empirically to be a function of field strength (H) to H^m and frequency (f) to f^n [26] where the values of m and n are experimentally determined. Fig. 5 shows the dependence on field strength can be fit to the mth order power-law curve, where at low field strengths $m = 2$ (dashed line), but at higher field strengths, $m = 3$ (dotted line).

Third-order power-law H dependences are typical of Rayleigh losses [27]. Previous work has shown that second-order losses are indicative of superparamagnetic samples and third order losses for ferromagnetic samples [18]. The phenomenon of switching from $m = 2$ to 3 field dependence has been observed in magnetic hystereses of magnetosomes [28] but this is not described by the power loss equation, which only shows a square law field dependence. Since we also observe this behavior, it suggests that hysteresis losses may play a role in the heating of the Fe-doped Au nanoparticles. Therefore, power losses alone cannot describe the frequency-and field-dependent behavior of these particles.

Optimum choice of f and H for hyperthermia can be determined empirically from the magnetic heating experiments of Fe-doped Au nanoparticles. Fig. 4a shows that increasing the field frequency above 40 MHz does not contribute significantly to the SAR losses. For this frequency, the hypothetical temperature rise depends on field strength H of the system. In the case of burning a tumor, raising the temperature to 42 °C has been found optimal [26]. Here we show that using an approximate field strength of 100 A/m is necessary to reach this temperature (Fig. 3). However, this case is for a solution of pure nanoparticles and use in clinical environments such as in

tissues would most likely require different field strengths. The frequency dependence of direct heating by magnetic field on different clinical environments may also influence the choice of optimum frequency [29].

3. Conclusions

We find that Fe-doped Au nanoparticles are suitable for magnetic heating, and thus have potential for use in hyperthermia applications. While SAR of the nanoparticles follows general trends for frequency dependence described by the power loss equation, the dependence on H does not quantitatively agree. Therefore, mechanisms other than Brownian and Néel losses are necessary to describe the heating behavior of these particles. The data suggests that hysteresis losses may be a factor, and further study is necessary. Fe-doped Au nanoparticles represent one step in expanding the set of materials utilized in hyperthermia and other magnetic field heating applications. Further studies of how magnetic heating is influenced by nanoparticle size and Fe content will be performed in future investigations.

Acknowledgements

This work was funded by the Office of Naval Research (N00014-04-1-0570). We are grateful to the Center for Materials Science for use of their SQUID and TEM.

References

[1] J.M. Perez, L. Josephson, T. O'Loughlin, D. Högemann, R. Weissleder, Nat. Biotechnol. 20 (2002) 816.
[2] Y.-M. Huh, et al., J. Am. Chem. Soc. 127 (2005) 12387.
[3] C.C. Berry, A.S.G. Curtis, J. Phys. D 36 (2003) R198.
[4] M. Shinkai, et al., J. Magn. Magn. Mater. 194 (1999) 176.
[5] T. Hyeon, et al., J. Phys. Chem. B 106 (2002) 6831;
T. Hyeon, S.S. Lee, J. Park, Y. Chung, H.B. Na, J. Am. Chem. Soc. 123 (2001) 12798;
S. Sun, et al., J. Am. Chem. Soc. 126 (2004) 273.
[6] R. Elghanian, J.J. Storhoff, R.C. Mucic, R.L. Letsinger, C.A. Mirkin, Science 277 (1997) 1078.
[7] L.R. Hirsch, et al., Proc. Natl. Acad. Sci. USA 100 (2003) 13549.
[8] K. Hamad-Schifferli, J.J. Schwartz, A. Santos, S. Zhang, J.M. Jacobson, Nature 415 (2002) 152.
[9] D. Zanchet, C.M. Micheel, W.J. Parak, D. Gerion, A.P. Alivisatos, Nano Lett. 1 (2001) 32.
[10] S. Park, K.A. Brown, K. Hamad- Schifferli, Nano Lett. 4 (2004) 1925.
[11] M.-E. Aubin, D.G. Morales, K. Hamad- Schifferli, Nano Lett. 5 (2005) 519.
[12] J.F. Hainfield, R.D. Powell, J. Histochem. Cytochem. 48 (2000) 471.
[13] S.-J. Cho, et al., J. Appl. Phys. 95 (2004) 6804;
M. Chen, S. Yamamuro, D. Farrell, S.A. Majetich, J. Appl. Phys. 93 (2003) 7551;
W.-R. Lee, et al., J. Am. Chem. Soc. 127 (2005) 16090.
[14] K.A. Brown, A. Wijaya, J.D. Alper, K. Hamad-Schifferli, submittedfor publication, 2005.
[15] J.W. Slot, H.J. Geuze, Eur. J. Cell Biol. 83 (1985) 87.
[16] J.J. Storhoff, et al., J. Am. Chem. Soc. 122 (2000) 4640.
[17] H. Okamoto, T.B. Massalski, L.J. Swartzendruber, P.A. Beck, Bull. Alloy Phase Diagrams 5 (1984) 592.
[18] R. Hiergeist, et al., J. Magn. Magn. Mater. 201 (1999) 420.
[19] M. Ma, et al., J. Magn. Magn. Mater. 268 (2004) 33.
[20] S. Park, Master's Thesis, MIT , 2004.
[21] R. Hergt, et al., IEEE Trans. Magn. 34 (1998) 3745.
[22] R.E. Rosensweig, J. Magn. Magn. Mater. 252 (2002) 370.
[23] A. Jordan, et al., Inter. J. Hyptherm. 9 (1993) 51.
[24] H. Landolt, R. Börnstein, Landolt–Börnstein Numerical Data and Functional Relationships in Science and Technology, New Series, vol. III/19b,Springer, Berlin, 1987.
[25] K. Takanashi, et al., Appl. Phys. Lett. 67 (1995) 1016.
[26] D.C.F. Chan, D.B. Kirpotin, P.A. Bunn, J. Magn. Magn. Mater. 122 (1993) 374.
[27] S. Chikazumi, Physics of Ferromagnetism, Oxford University Press, Oxford, 1997.
[28] R. Hergt, et al., J. Magn. Magn. Mater. 293 (2005) 80.
[29] I.A. Brezovich, Medical Physics Monograph 16 (1988) 82.